Analytical vs Numerical Solutions in Magnetohydrodynamics

CAMK Summer Internship Report

Borishan Ghosh

August 2024

Contents

1 Introduction

The problem of solving systems of nonlinear hyperbolic conservation laws is stated as follows,

$$\partial_t \mathbf{U} + \partial_x \mathbf{F}(\mathbf{U}) = 0 \tag{1}$$

Where $\mathbf{U}$ stands for a conserved quantity as a function of space and time and $\mathbf{F}$ is a smooth function on $\mathbf{U}$ denoting flux.

Various methods exist to solve the same numerically for discrete points in space and time. In this report, we examine a few popular methods in solving specifically the Euler equations for linearized gas dynamics in 1D [1].

$$\mathbf{U} = \begin{bmatrix} \rho \\ m \\ E \end{bmatrix}, \quad \mathbf{F} = \begin{bmatrix} m \\ \rho u^2 + p \\ u(E+p) \end{bmatrix}, \quad \text{with} \quad p = (\gamma - 1)\left(E - \frac{\rho}{2}u^2\right) \tag{2}$$

2 Sod problem

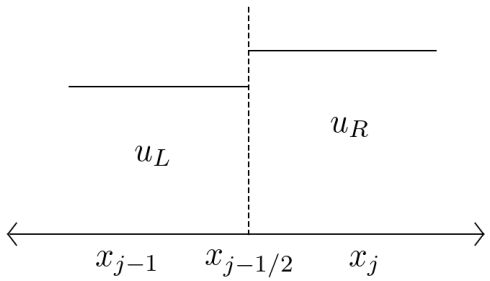

Figure 1: Riemann Problem

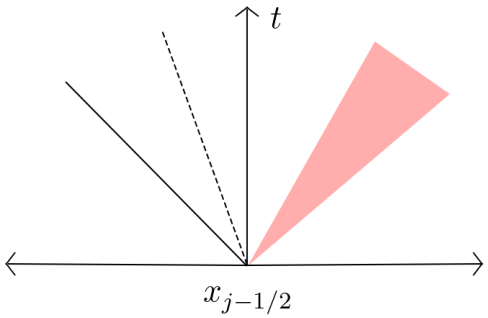

Figure 2: Evolution of a shock with the shock-wave (solid line), contact discontinuity (dotted), rarefaction wave (shaded)

The setup for a Riemann Problem is a discontinuity(i.e. a shock) across an interface written in terms of the left and right states $(\mathbf{u}_L, \mathbf{u}_R)$. The exact solutions for some such problems are known. One proposed by Sod in [2] is used as to benchmark for numerical schemes.

$$\mathbf{u}_L = \begin{bmatrix} 1 \\ 0 \\ 2.5 \end{bmatrix}, \quad \mathbf{u}_R = \begin{bmatrix} 0.125 \\ 0 \\ 0.25 \end{bmatrix}$$

The "shocktube" can be divided into a mesh of N points $\{x_i\}$ with $x_i = x_0 + (i-1)\cdot\Delta x$ and $i = 1, 2, \ldots N$ and $t_j = (j-1)\cdot\Delta t$ for some positive integer j. Given an approximate solution at a time t_n written $\mathbf{u}(x_i, t_n) \approx \mathbf{u}_i^n$, the scheme L provides the update $\mathbf{u}_i^{n+1} = L\mathbf{u}_i^n$.

3 Outline of Methods

3.1 Overview

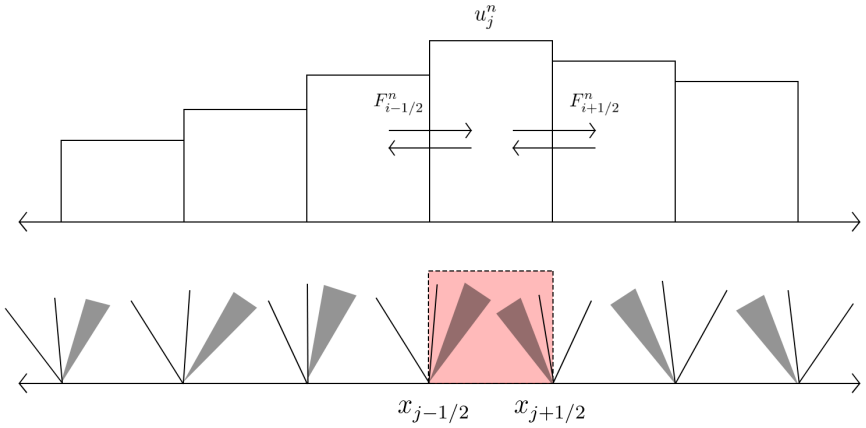

Figure 3: Integrating over the shaded region gives an expression for flux at each discontinuous boundary

Starting with the general form for the conservation equation we can integrate over the domain $[x_{i-1/2}, x_{i+1/2}] \times [t, t + \Delta t]$,

$$\int_t^{t+\Delta t} \int_{x_{i-1/2}}^{x_{i+1/2}} \left(\frac{\partial}{\partial t} \mathbf{u}(x,t) + \frac{\partial}{\partial x} f(\mathbf{u}(x,t)) \right) \, dx \, dt = 0 \quad \text{where,} \quad x_{i+1/2} = x_i + \frac{\Delta x}{2} \tag{3}$$

Assuming that $\mathbf{u}(x,t)$ and its corresponding flux is well behaved,

$$\int_{x_{i-1/2}}^{x_{i+1/2}} \mathbf{u}(x, t + \Delta t) \, dx = \int_{x_{i-1/2}}^{x_{i+1/2}} \mathbf{u}(x,t) \, dx - \int_t^{t+\Delta t} (f(\mathbf{u}(x_{i+1/2}, t)) - f(\mathbf{u}(x_{i-1/2}, t))) \, dt \tag{4}$$

The cell averages are defined,

$$\bar{\mathbf{u}}_i^n := \frac{1}{\Delta x} \int_{x_{i-1/2}}^{x_{i+1/2}} \mathbf{u}(x, t_n) \, dx$$

Writing (4) in terms of cell averages,

$$\bar{\mathbf{u}}_i^{n+1} = \bar{\mathbf{u}}_i^n - \frac{1}{\Delta x} \int_{t^n}^{t^{n+1}} (f(\mathbf{u}(x_{i+1/2}, t)) - f(\mathbf{u}(x_{i-1/2}, t))) \, dt \tag{5}$$

Various Godunov-type schemes replace the flux integral term with an exact solution or an approximation of the Riemann problem. The scheme thus takes the general form,

$$\bar{\mathbf{u}}_i^{n+1} = \bar{\mathbf{u}}_i^n - \frac{\Delta t}{\Delta x} (F_{i+1/2} - F_{i+1/2}) \tag{6}$$

3.2 Godonov Scheme

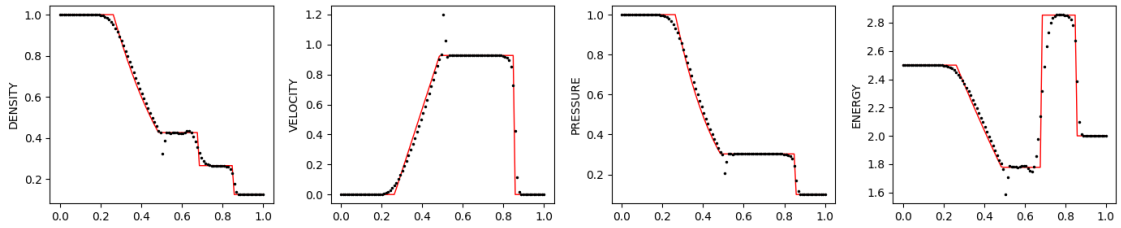

Figure 4: Sod Problem evaluated with the Godunov Scheme with N = 100, t = 0.2

In Sod's review of methods, a simplified form of a Riemann solver is considered where $F_{i+1/2} \approx \mathbf{F}(\mathbf{u}^{n+1}_{i+1/2})$. $\mathbf{u}^{n+1}_{i+1/2}$ is an approximation of the conserved quantity at the following time-step. The update is as follows,

$$\bar{\mathbf{u}}^{n}_{i+1/2} = \frac{1}{2}(\mathbf{u}^{n}_{i+1} + \mathbf{u}^{n}_{i}) + \frac{\Delta t}{\Delta x}(\mathbf{F}^{n}_{i+1} - \mathbf{F}^{n}_{i}) \tag{7}$$

$$\mathbf{u}^{n+1}_{i} = \mathbf{u}^{n}_{i} - \frac{\Delta t}{\Delta x}(\bar{\mathbf{F}}^{n+1}_{i+1/2} - \bar{\mathbf{F}}^{n+1}_{i-1/2}) \tag{8}$$

Note the discontinuities at the initial shock point of $x = 0.5$, this spiking behaviour is aggravated with higher values of N, and are not resolved in similar schemes such as the Lax-Wendroff method. The spikes disappear when an artificial viscosity correction is applied.

3.3 Lax Wendroff Scheme

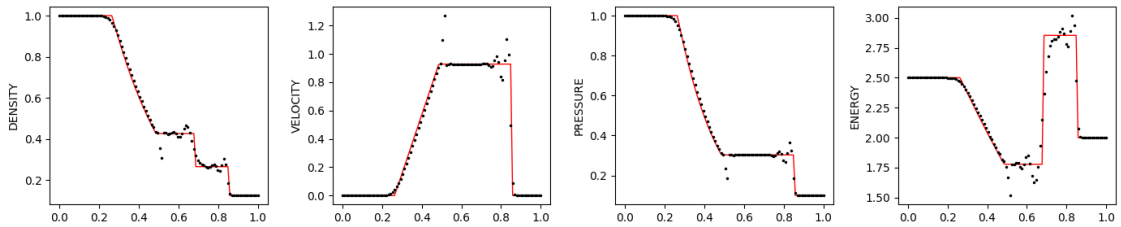

Figure 5: Sod Problem evaluated with the Lax Wendroff Scheme with N = 100, t = 0.2

The Lax-Wendroff Scheme described in Sod is one of the alternative two step methods developed by Richtmyer in [4] It is 2nd order accurate with the expression for cell interfaces resembling the one in the Godunov step.

$$\mathbf{u}^{n+1/2}_{i+1/2} = \frac{1}{2}(\mathbf{u}^{n}_{i+1} + \mathbf{u}^{n}_{i}) + \frac{\Delta t}{2\Delta x}(\mathbf{F}^{n}_{i+1} - \mathbf{F}^{n}_{i}) \tag{9}$$

$$\mathbf{u}^{n+1}_{i} = \mathbf{u}^{n}_{i} - \frac{\Delta t}{\Delta x}(\mathbf{F}^{n+1/2}_{i+1/2} - \mathbf{F}^{n+1/2}_{i-1/2}) \tag{10}$$

The Lax Wendroff being a 2nd order scheme exhibits oscillations near the discontinuities as compared to the 1st order Godunov Scheme in Figure 4.

3.4 MacCormack Scheme

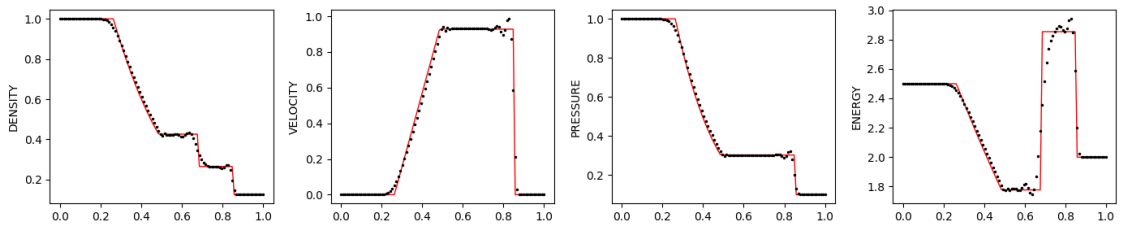

Figure 6: Sod Problem evaluated with the MacCormack Scheme with N = 100, t = 0.2 and AV $\nu = 1$

Similar to Richtmyer procedure, this scheme is another one of the modifications to the Lax-Wendroff Scheme given by MacCormack [5].

$$\bar{\mathbf{u}}_i^{n+1} = \mathbf{u}_i^n - \frac{\Delta t}{\Delta x}(F_{i+1}^n - F_i^n) \tag{11}$$

$$\mathbf{u}_i^{n+1} = \frac{1}{2}(\mathbf{u}_i^n + \bar{\mathbf{u}}_i^{n+1} - \frac{\Delta t}{\Delta x}(\bar{F}_i^{n+1} - \bar{F}_{i-1}^{n+1})) \tag{12}$$

It is a combination of a Predictor step that uses 1st order forward differencing and a Corrector step that uses 1st order backward differencing, the update essentially averages the effect of the two approximate derivatives.

The MacCormack Scheme is a 2nd order scheme that does not converge on its own given the initial conditions in Sod's Paper. It however performs well along with the incorporation of artificial velocity.

3.5 Rusanov Scheme

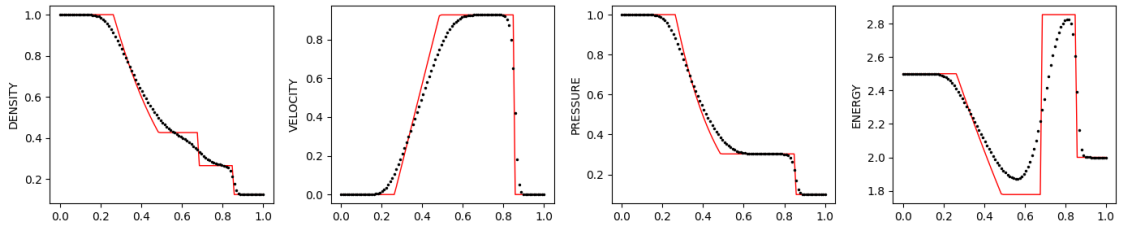

Figure 7: Sod Problem evaluated with the Rusanov Scheme with N = 100, t = 0.2 and $\omega = 1$

The scheme described by Rusanov in his original paper is as follows [3],

$$\mathbf{u}_i^{n+1} = \mathbf{u}_i^n - \frac{\Delta t}{2\Delta x}(F_{i+1}^n - F_{i-1}^n) + \frac{1}{2}(\Phi_{i+1/2} - \Phi_{i-1/2}) \tag{13}$$

Where,

$$\Phi_{i+1/2} = \frac{1}{2}(\alpha_{i+1}^n + \alpha_i^n)(\mathbf{u}_{i+1}^n - \mathbf{u}_i^n) \tag{14}$$

$$\alpha_i^n = \omega\frac{\Delta t}{\Delta x}(u + c)_i^n \tag{15}$$

Here, u is the velocity variable and c the local sound speed. The scheme is of 1st order and generally performs better with artificial compression.

3.6 Hyman Scheme

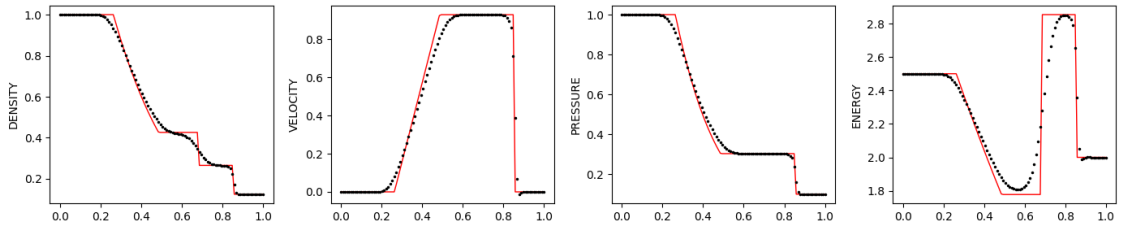

Figure 8: Sod Problem evaluated with the Hyman Scheme with N = 100, t = 0.2 and $\delta = 0.8$

The Hyman scheme is based on a predictor-corrector model similar to the MacCormack Scheme. The $\phi^n_{i+1/2}$ term much like the Rusanov Scheme acts to supply artificial viscosity in order to maintain stability and to insure proper entropy production.

$$\mathbf{u}_i^{n+1/2} = \mathbf{u}_i^n - \Delta t \mathbf{P}_i^n \tag{16}$$

$$\mathbf{u}_i^{n+1} = \mathbf{u}_i^n - \frac{\Delta t}{2}(D\mathbf{F}_i^{n+1/2} + \mathbf{P}_i^n) \tag{17}$$

Where,

$$\mathbf{P}_i^n = D\mathbf{F}_i^n - \delta(\phi^n_{1-1/2} - \phi^n_{i-1/2}) \tag{18}$$

$$D\mathbf{F}_i^n = \frac{1}{12\Delta x}(-\mathbf{F}^n_{i+2} + 8\mathbf{F}^n_{i+1} - 8\mathbf{F}^n_{i-1} + \mathbf{F}^n_{i-2}) \tag{19}$$

$$\phi^n_{i+1/2} = \frac{1}{4\Delta x}(\alpha^n_{i+1} - \alpha^n_i)(\mathbf{u}^n_{i+1} - \mathbf{u}^n_i) \tag{20}$$

$$\alpha^n_i = (u + c)^n_i \tag{21}$$

Here, the artificial viscosity term can be reduced in smooth regions with the help of a "switch", replacing $\phi^n_{i+1/2}$ by $\beta\phi^n_{i+1/2}$ where,

$$\beta = \begin{cases} \frac{1}{3}, & \text{if } \alpha^n_{i+1} > \alpha^n_i + \frac{\Delta x}{3} \\ 1, & \text{otherwise.} \end{cases}$$

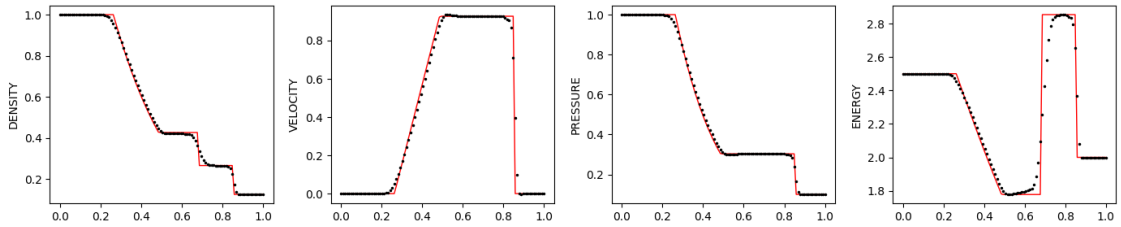

Figure 9: Hyman Scheme with similar parameters and switch enabled.

The smearing of discontinuities are hence greatly reduced.

3.7 Hybrid Schemes

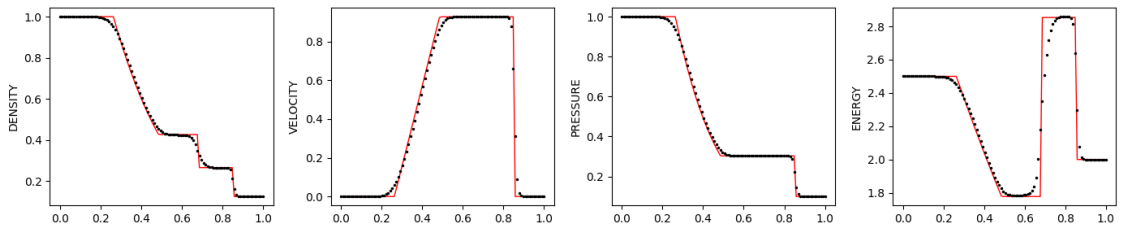

Figure 10: Sod Problem evaluated with the Hybrid Scheme with N = 100, t = 0.2

Given a 1st order scheme (L_1) and a kth order scheme (L_k) we would like to interpolate the same so that the non-oscillatory characteristics of the 1st order scheme is maintained over the discontinuities, while the higher order scheme is applied over smooth regions.

$$L_1\mathbf{u}_i = \mathbf{u}_i - \frac{\Delta t}{\delta x}(f^1_{i+1/2} - f^1_{i-1/2}) \tag{22}$$

$$L_k\mathbf{u}_i = \mathbf{u}_i - \frac{\Delta t}{\delta x}(f^k_{i+1/2} - f^k_{i-1/2}) \tag{23}$$

This gives rise to a "hybridized" scheme from the L_1 and L_k operators.

$$L\mathbf{u}_i = \mathbf{u}_i - \frac{\Delta t}{\delta x}(f_{i+1/2} - f_{i-1/2}) \tag{24}$$

where,

$$f_{i+1/2} = \theta_{i+1/2}f^1_{i+1/2} + (1 - \theta_{i+1/2})f^k_{i+1/2} \tag{25}$$

Here $\theta_{i+1/2}$ is a "switch" that lies in the range $[0, 1]$ and approaches 1 near discontinuities. Beginning with the MacCormack Scheme(2nd order), Sod introduces a artificial viscosity term to obtain the 1st order scheme.

$$\bar{\mathbf{u}}^{n+1}_i = \mathbf{u}^n_i - \frac{\Delta t}{\Delta x}(\mathbf{F}^n_{i+1} - \mathbf{F}^n_i) \tag{26}$$

$$\mathbf{u}^{n+1}_i = \frac{1}{2}(\mathbf{u}^{n+1}_i - \mathbf{u}^n_i) - \frac{\Delta t}{2\Delta x}(\bar{\mathbf{F}}^{n+1}_i - \bar{\mathbf{F}}^{n+1}_{i-1}) \tag{27}$$

$$+ \frac{1}{8}\theta^n_{i+1/2}(\mathbf{u}^n_{i+1} - \mathbf{u}^n_i) - \theta^n_{i-1/2}(\mathbf{u}^n_i - \mathbf{u}^n_{i-1}) \tag{28}$$

The θ switch used here is based on differences in the density profile,

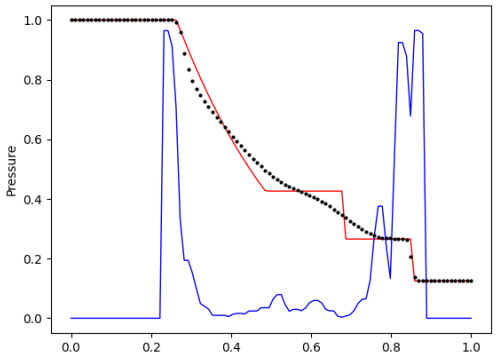

Figure 11: Hybrid Switch evaluated after a Rusanov update step, t = 0.2

$$\theta^n_{i+1/2} = \max(\theta^n_i, \theta^n_{i+1}) \tag{29}$$

$$\theta^n_i = \begin{cases} \left| \frac{|\Delta_{i+1/2}| - |\Delta_{i-1/2}|}{|\Delta_{i+1/2}| + |\Delta_{i-1/2}|} \right| & \text{if, } |\Delta_{i+1/2}| + |\Delta_{i-1/2}| > \epsilon \\ 0, & \text{otherwise} \end{cases} \tag{30}$$

$$\Delta_{i+1/2} = \rho_{i+1} - \rho_i \tag{31}$$

3.8 Antidiffusion method

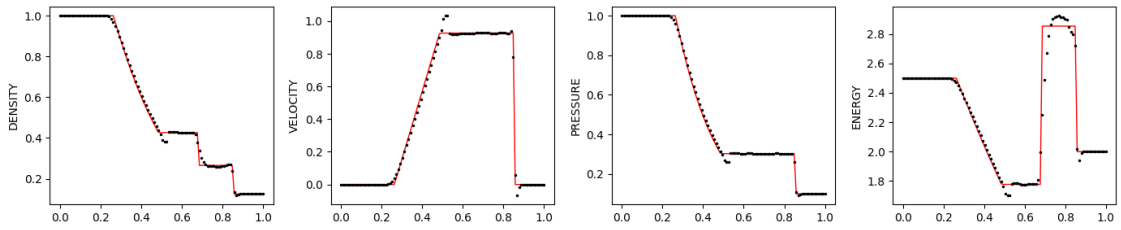

Figure 12: Sod Problem evaluated with the Antidiffusion Method with N = 100, t = 0.2

The antififfusion method of Boris and Book is an example of "flux correction". Starting with the Lax Wendroff Procedure described above obtaining $\tilde{\mathbf{u}}^{n+1}_i$, we apply the antidiffusion step,

$$\hat{\mathbf{u}}^{n+1}_i = \tilde{\mathbf{u}}^{n+1}_i + \eta(\mathbf{u}^n_{i+1} - 2\mathbf{u}^n_i + \mathbf{u}^n_{i-1}) \tag{32}$$

$$\mathbf{u}^{n+1}_i = \hat{\mathbf{u}}^{n+1}_i - (f^c_{i+1/2} - f^c_{i-1/2}) \tag{33}$$

where,

$$\hat{\Delta}_{i+1/2} = \eta(\tilde{\mathbf{u}}^{n+1}_{i+1} - \tilde{\mathbf{u}}^{n+1}_i) \tag{34}$$

$$\Delta_{i+1/2} = \hat{\mathbf{u}}^{n+1}_{i+1} - \hat{\mathbf{u}}^{n+1}_i \tag{35}$$

$$f^c_{i+1/2} = \text{sgn}(\hat{\Delta}_{i+1/2}) \max[0, \min[\text{sgn}(\hat{\Delta}_{i+1/2}\Delta_{i-1/2}, |\hat{\Delta}_{i+1/2}|, \text{sgn}(\hat{\Delta}_{i+1/2})\Delta_{i+3/2}] \tag{36}$$

The parameter η is the diffusion/antidiffusion coefficient. The method thus obtains high resolution without much oscillations.

3.9 Artificial Viscosity

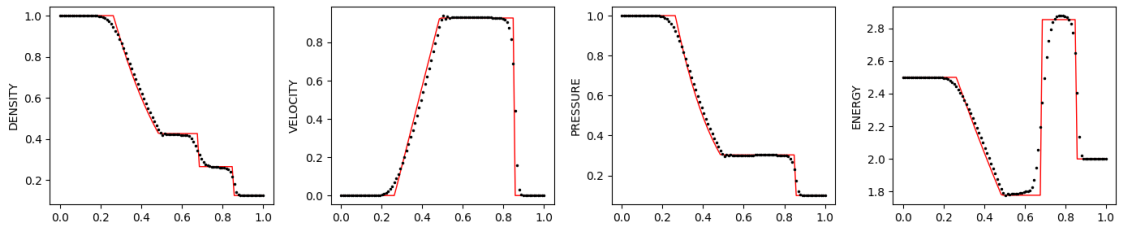

Figure 13: Godunov Scheme with N = 100, t = 0.2 and AV $\nu = 1$

The artificial viscosity term is incorporated to stabilize the various schemes present in Sod's paper. It is a simple correction applied at the end of each update to diffuse anomalous discontinuities.

Given an update $\tilde{\mathbf{u}}^{n+1}_i$, we replace the approximation by,

$$\mathbf{u}^{n+1}_i = \tilde{\mathbf{u}}^{n+1}_i + \frac{\nu \Delta t}{\Delta x} \Delta'[\Delta' \tilde{u}^{n+1}_{i+1} \cdot \Delta' \tilde{\mathbf{u}}^{n+1}_{i+1}] \tag{37}$$

Where Δ' denotes difference from the left boundary (for example, $\Delta' \tilde{u}^{n+1}_{i+1} = \tilde{u}^{n+1}_{i+1} - \tilde{u}^{n+1}_i$) and ν is an adjustable parameter set to 1 for the demonstrations in this report.

3.10 Artificial Compression

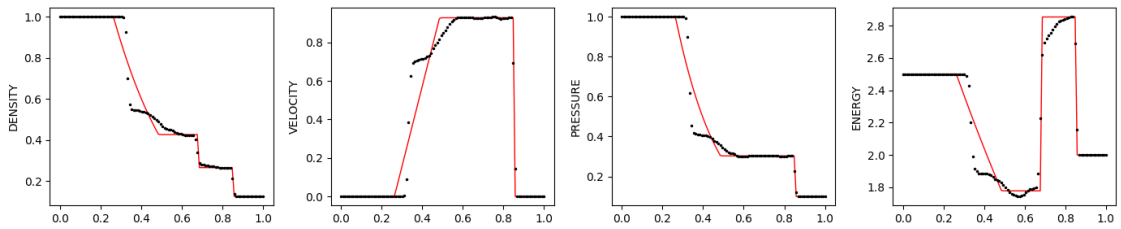

Figure 14: Rusanov Scheme with N = 100, t = 0.2 and ACM $\hat{\lambda} = 1$

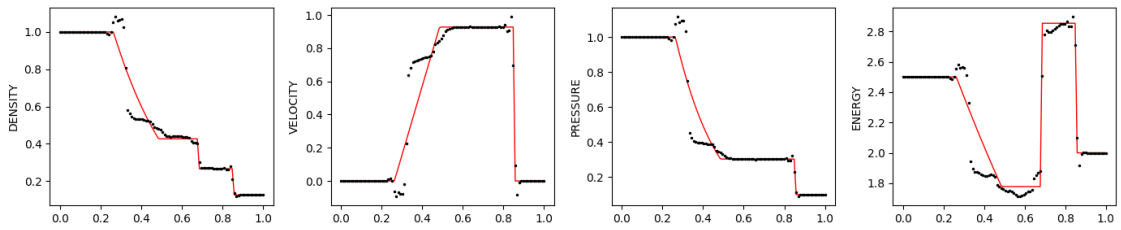

Figure 15: Hyman Scheme with N = 100, t = 0.2 and ACM $\hat{\lambda} = 1$

Artificial Compression, first introduced by Harten in [6], is a method used to sharpen regions of discontinuities such as those of shocks or contact discontinuities.

Starting with the updated $\tilde{\mathbf{u}}_i^{n+1}$, we apply the following update,

$$\mathbf{u}_i^{n+1} = \tilde{\mathbf{u}}_i^{n+1} - \frac{\hat{\lambda}}{2}(\mathbf{G}_{i+1/2}^n - \mathbf{G}_{i-1/2}^n) \tag{38}$$

where,

$$\mathbf{G}_{i+1/2}^n = \mathbf{g}_i^n - \mathbf{g}_{i+1}^n - |\mathbf{g}_i^n - \mathbf{g}_{i+1}^n|\mathbf{S}_{i+1/2} \tag{39}$$

$$\mathbf{S}_{i+1/2,k} = \text{sgn}(\delta_{i-1/2}^k) \tag{40}$$

$$\delta_{i+1/2}^k = \tilde{\mathbf{u}}_{i+1}^{(k)} - \tilde{\mathbf{u}}_i^{(k)} \tag{41}$$

$$\mathbf{g}_i = \alpha_i \Delta_i \tag{42}$$

$$\Delta_i = \tilde{\mathbf{u}}_{i+1} - \tilde{\mathbf{u}}_i \tag{43}$$

$$\alpha = \max\left\{0, \min_k\left[\frac{\min(|\delta_{i+1/2}^k|, \delta_{i-1/2}^k) \cdot \text{sgn}(\delta_{i+1/2}^k)}{|\delta_{i+1/2}^k| + |\delta_{i-1/2}^k|}\right]\right\} \tag{44}$$

The denominator within Equation(44), can sometimes equal zero in which case the resulting value of α is 0 as well, however such cases must be dealt with separately in computer implementations.

Harten explicitly sets $\hat{\lambda} = 1$, in his paper however Sod replaces the term in Equation (38) with $\Delta t/\Delta x$, this makes the ACM update weaker albeit effective.

To prevent the use of ACM near smooth regions, we can utilize the θ switch introduced in the hybrid scheme, replacing (38) with

$$\mathbf{u}_i^{n+1} = \tilde{\mathbf{u}}_i^{n+1} - \frac{\hat{\lambda}}{2}(\theta_{i+1/2}^n \mathbf{G}_{i+1/2}^n - \theta_{i-1/2}^n \mathbf{G}_{i-1/2}^n) \tag{45}$$

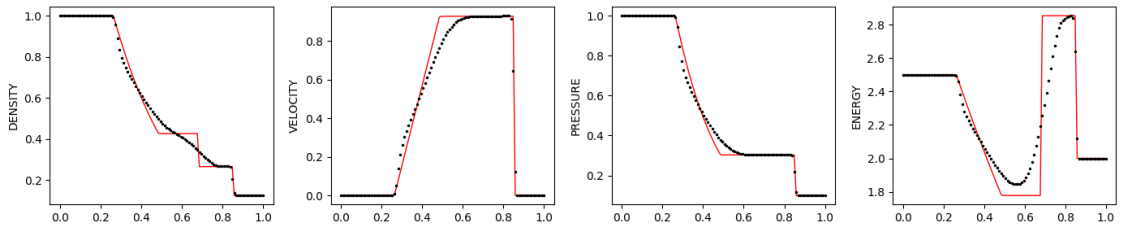

Figure 16: Rusanov Scheme with N = 100, t = 0.2 and ACM $\hat{\lambda} = 1$ with hybrid switch

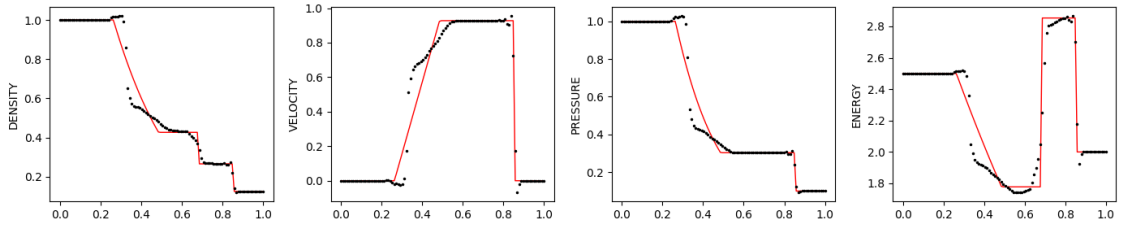

Figure 17: Hyman Scheme with N = 100, t = 0.2 and ACM $\hat{\lambda} = 1$ with hybrid switch

4 Kurganov and Tadmor Central Scheme

4.1 Overview

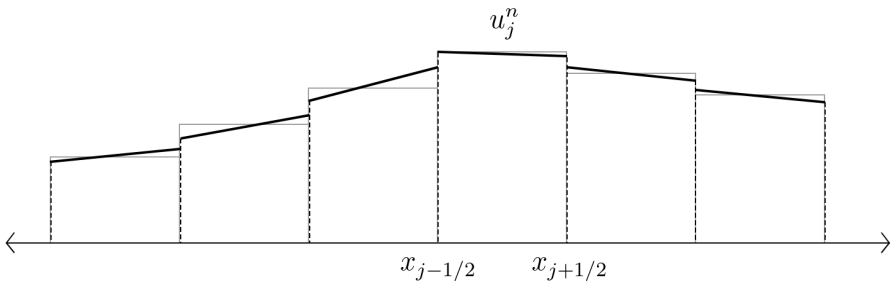

Figure 18: a piece-wise linear approximation of $u(x,t)$

The central scheme introduced by Lax and Fredrichs in 1954 proposes a simple first-order accurate alternative to Godunov schemes that is free of Riemann solvers.

$$u_i^{n+1} = \frac{1}{2}(u_{i+1}^n - u_{i-1}^n) - \frac{\lambda}{2}(f(u_{i+1}^n) - f(u_{i-1}^n)) \tag{46}$$

The LxF scheme however is relatively diffusive and lacks sharp resolutions of discontinuities and rarefaction tips. The Nessyahu-Tadmor scheme is a higher order extension of the same that replaces the piece-wise constant approximation of the discretized conserved quantity to a piece-wise linear second-order approximation.

$$\tilde{u}(x,t) := \sum_i [\bar{u}_i^n + (u_x)_i^n (x - x_i)] \mathbf{1}_{[x_{i-1/2}, x_{i+1/2}]} \tag{47}$$

Where, $\{\bar{u}_j^n\}$ are the cell averages and $\{(u_x)_j^n\}$ are the approximate derivatives that are reconstructed from the cell averages. A total-variation diminishing reconstruction can be obtained from a minmod flux limiter defined as so,

$$(u_x)_i^n = \text{minmod}\left(\frac{u_i^n - u_{i-1}^n}{\Delta x}, \frac{u_{i+1}^n - u_i^n}{\Delta x}\right) \tag{48}$$

The minmod function is defined $\text{minmod}(a,b) := \frac{1}{2}[\text{sgn}(a)+\text{sgn}(b)]\min(|a|,|b|)$. The linear approximation remains smooth around points $\{x_i\}$ for sufficiently fine Δt, however it may be discontinuous at the interfaces.

Solving for the terms in (5) we can find $\bar{\mathbf{u}}(x,t)$ in the RHS by integrating (47) over $[x_i, x_{i+1}]$, the flux integral are approximated by midpoint rule, this gives the NT scheme [7].

$$\bar{u}^{n+1}_{i+1/2} = \frac{1}{2}(\bar{u}^n_i + \bar{u}^n_{i+1}) + \frac{\Delta x}{8}((u_x)^n_i - (u_x)^n_{i+1}) - \lambda(f(u^{n+1/2}_{i+1}) - f(u^{n+1/2}_i)) \tag{49}$$

Where, $u^{n+1/2}_i$ is given by the taylor approximation,

$$u^{n+1/2}_i = \bar{u}^n_i - \frac{\Delta t}{2}(f_x)^n_i \tag{50}$$

4.2 1D Fully Discrete Setup

We begin by finding the maximal local speed of propagation at cell interfaces, denoted $a^n_{i+1/2}$. This value is found in practice by finding the spectral radius of the flux jacobian $\partial f/\partial u$ at the left and right values of the approximate $\tilde{u}(x,t_n)$ at $x_{i+1/2}$.

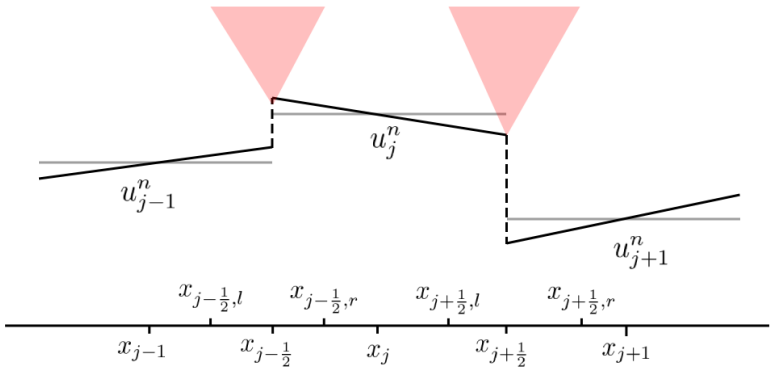

Figure 19: Due to finite speed of propagation the control volume is restricted to $[x_{i+1/2,l}, x_{i+1/2,r}] \times [t_n, t_{n+1}]$

The intermediate values are defined $u^+_{i+1/2} := u^n_{i+1} - \frac{\Delta x}{2}(u_x)^n_{i+1}$ and $u^-_{i+1/2} := u^n_i + \frac{\Delta x}{2}(u_x)^n_i$. The speeds are hence given by,

$$a^n_{i+1/2} := \max\left[\rho\left(\frac{\partial f}{\partial u}(u^+_{i+1/2})\right), \rho\left(\frac{\partial f}{\partial u}(u^-_{i+1/2})\right)\right] \tag{51}$$

We can thus reduce the volume of integration to a much finer $[x_{i+1/2,l}, x_{i+1/2,r}] \times [t_n, t_{n+1}]$ where $x_{i+1/2,l} := x_i + 1/2 - a_{j+1/2}\Delta t$ and $x_{i+1/2,r} := x_i + 1/2 + a_{j+1/2}\Delta t$. We can perform the same procedure as in equation (4) integrating over the updated limits. The flux integrals are approximated by midpoint rule, doing so requires the new cell averages $\{w^{n+1}_i\}$ and the same at the interfaces $\{w^{n+1}_{i+1/2}\}$ evaluated as so,

$$\begin{aligned} w^{n+1}_{i+1/2} &= \frac{u^{n+1}_i + u^n_i}{2} + \frac{\Delta x - a^n_{i+1/2}\Delta t}{4}((u_x)^n_i - (u_x)^n_{i+1}) \\ &\quad - \frac{1}{2a^n_{i+1/2}}[f(u^{n+1/2}_{i+1/2,r}) - f(u^{n+1/2}_{i+1/2,l})] \end{aligned} \tag{52}$$

$$\begin{aligned} w^{n+1}_i &= u^n_i + \frac{\Delta t}{2}(a^n_{i-1/2} - a^n_{i+1/2})(u_x)^n_i \\ &\quad - \frac{\lambda}{1-\lambda(a^n_{i-1/2} + a^n_{i+1/2})}[f(u^{n+1/2}_{i+1/2,l}) - f(u^{n+1/2}_{i-1/2,r}] \end{aligned} \tag{53}$$

Where the midpoint values are given by their respective Taylor approximations,

$$u^{n+1/2}_{i+1/2,l} := u^n_{i+1/2,l} - \frac{\Delta t}{2} f(u^n_{i+1/2,l})_x, \qquad u^n_{i+1/2,l} := u^n_i + \Delta x (u_x)^n_i (\frac{1}{2} - \lambda a^n_{i+1/2}) \tag{54}$$

$$u^{n+1/2}_{i+1/2,r} := u^n_{i+1/2,r} - \frac{\Delta t}{2} f(u^n_{i+1/2,r})_x, \qquad u^n_{i+1/2,r} := u^n_{i+1} - \Delta x (u_x)^n_{i+1} (\frac{1}{2} - \lambda a^n_{i+1/2}) \tag{55}$$

The flux terms f_x can be computed exactly from the flux jacobians as well as component-wise from the cell averages, it can be shown that both yield effectively the sane results.

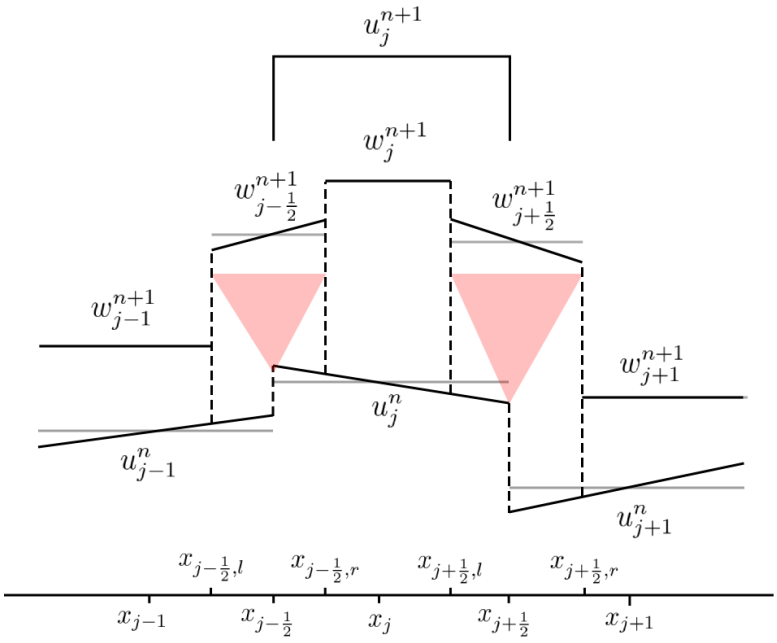

Figure 20: Integrating $\tilde{w}(x,t)$ over $[x_{i-1/2}, x_{i+1/2}]$ gives the final cell update

The reconstructed intermediate approximation is written,

$$\tilde{w}(x,t) := \sum_i \{[w^{n+1}_{i+1/2} + (u_x)^{n+1/2}_{i+1/2}(x - x_{i+1/2})\mathbf{1}_{[x^n_{i+1/2,l}, x^n_{i+1/2,r}]}] + w^{n+1}_i \mathbf{1}_{[x^n_{i-1/2,r}, x^n_{i+1/2,l}]}\} \tag{56}$$

The approximate derivatives here are once again computed with the help of the minmod limiters,

$$(u_x)^{n+1}_{i+1/2} = \frac{2}{\Delta x} \text{minmod}\left(\frac{w^{n+1}_{i+1} - w^{n+1/2}_{i+1/2}}{1 + \lambda(a^n_{i+1/2} - a^n_{i+3/2})}, \frac{w^{n+1}_{i+1/2} - w^{n+1/2}_i}{1 + \lambda(a^n_{i+1/2} - a^n_{i-1/2})} \right) \tag{57}$$

Finally, the fully-discrete second-order formulation is as follows [8],

$$\begin{aligned} u^{n+1}_i &= \frac{1}{\Delta x} \int_{x_{i-1/2}}^{x_{i+1/2}} \tilde{w}(\xi, t_{n+1}) d\xi \\ &= \lambda a^n_{i-1/2} w^{n+1}_{i-1/2} + [1 - \lambda(a^n_{i-1/2} + a^n_{i+1/2})] w^{n+1}_i \\ &+ \lambda a^n_{i+1/2} w^{n+1}_{i+1/2} + \frac{\Delta x}{2} [(\lambda a^n_{i-1/2})^2 (u_x)^{n+1}_{i-1/2} - (\lambda a^n_{i+1/2})^2 (u_x)^{n+1}_{i+1/2}] \end{aligned} \tag{58}$$

4.3 Results

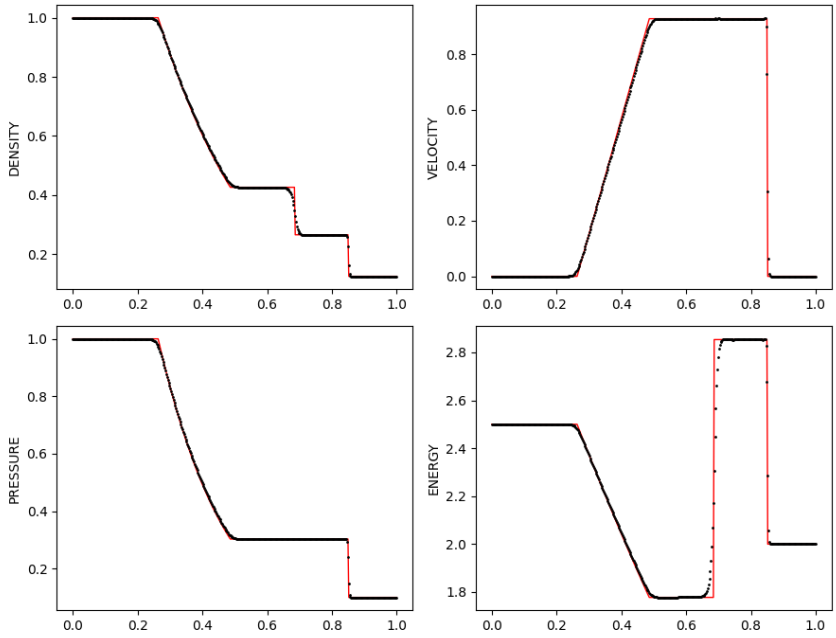

Figure 21: FD2 Scheme Evaluated on the Sod Problem with N = 400, T = 0.2

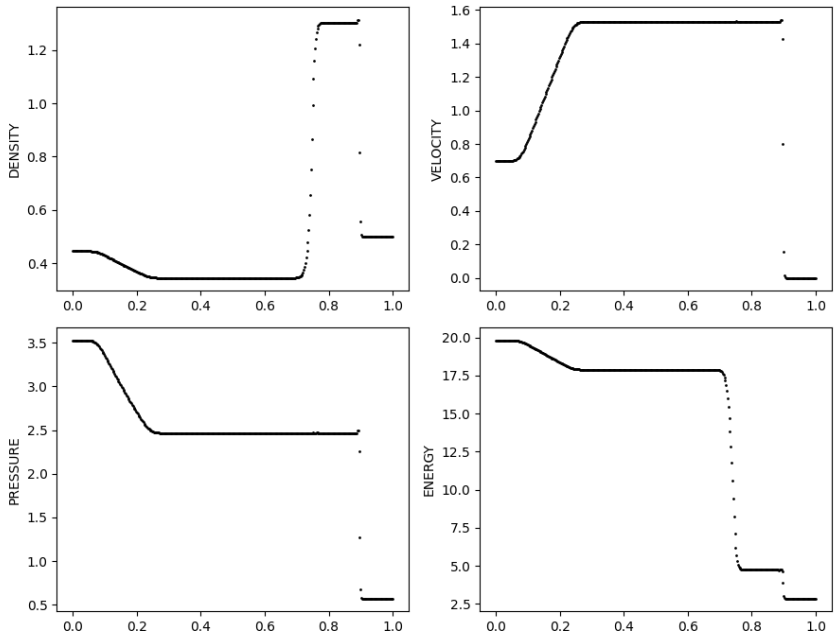

Figure 22: FD2 Scheme Evaluated on the Lax Problem with N = 400, T = 0.16

Setting the slopes of both $(u_x)_i^n$ and $(u_x)_{i+1/2}^{n+1}$ to zero in the reconstructed $w_{i+1/2}^{n+1}$ and w_i^{n+1}, we get the first order Rusanov Scheme,

$$u_i^{n+1} = u_i^n - \frac{\lambda}{2}[f(u_{i+1}^n) - f(u_{i-1}^n)] + \frac{\lambda}{2}[a_{i+1/2}^n(u_{i+1}^n - u_i^n) - a_{i-1/2}^n(u_i^n - u_{i-1}^n)] \tag{59}$$

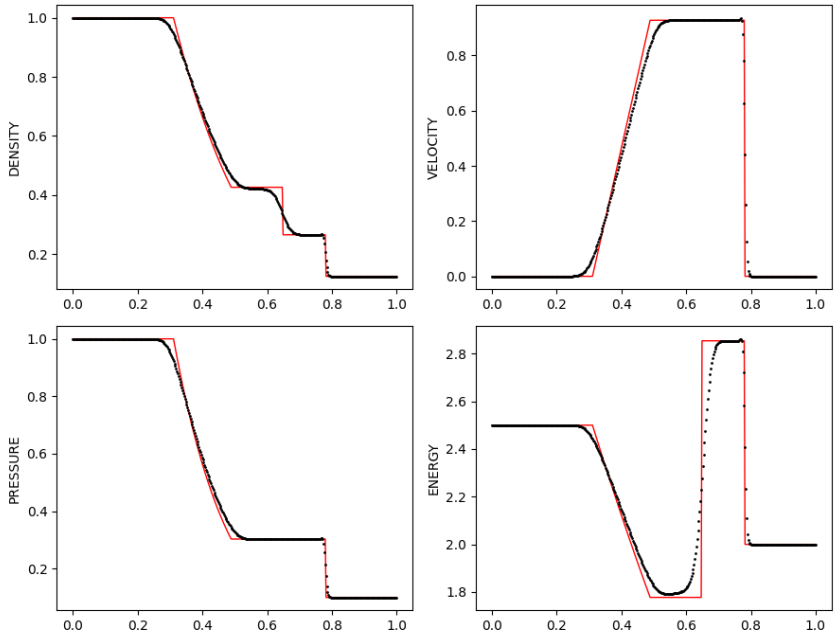

Figure 23: Rusanov Scheme from KT FD2 Scheme evaluated on the Lax Problem with N = 400, T = 0.2

5 Appendix

5.1 1D Riemann Problem Exact Solution

As an example of a Riemann problem suggested by Sod, we consider the case of discontinuous states $\mathbf{U}_L = (\rho_L, u_L, P_L)^T$ and $\mathbf{U}_R = (\rho_R, u_R, P_R)^T$ that is at rest at both sides of the discontinuity at $x = x_0$, i.e. $u_L = u_R = 0$. As time progresses this gives rise to 4 distinct regions within the shock tube. The following is a summary of the analysis presented by Lora-Clavijo et al. in [9].

Region 1 and 5 to the left and right-most ends of the tube where the shock and rarefaction waves have not propagated yet. The state at either end is the same as the initial condition. Supposing the case where the shock wave propagates to the right and the simultaneous rarefaction wave moves to the left, Region 2 corresponds to the Rarefaction wave. Region 3 and 4 are separated by a contact discontinuity. The shock separates Region 4 from 5.

5.1.1 Undisturbed Regions

Region 1 is given by $x - x_0 < tV_{\text{head}}$ where $V_{\text{head}} = u_L - a_1$ is the velocity of the head of the rarefaction wave. $a_1 = \sqrt{\gamma P_L/\rho_L}$ is simply the local speed of sound in Region 1. Similarly, Region 5 is given by $x - x_0 > tV_{\text{shock}}$ where V_{shock} is the velocity of shock wave described in the later sections.

$$\begin{aligned} \rho_1 &= \rho_L, \quad \rho_5 = \rho_R \\ u_1 &= u_L, \quad u_5 = u_R \\ P_1 &= P_L, \quad P_5 = P_R \end{aligned}$$

5.1.2 Rarefaction waves

Region 2 is defined $tV_{\text{head}} < x - x_0 < tV_{\text{tail}}$ with $V_{\text{tail}} = u_3 - a_3$ where a_3 is the local speed $\sqrt{\gamma P_3/\rho_3}$. The region forms a Riemann fan of varying characteristics,

$$\rho_3 = \rho_1 \left[\frac{2}{\gamma - 1} + \frac{\gamma - 1}{a_1(\gamma + 1)} \left(u_1 - \frac{x - x_0}{t} \right) \right]^{\frac{2}{\gamma - 1}} \tag{60}$$

$$P_3 = P_1 \left[\frac{2}{\gamma - 1} + \frac{\gamma - 1}{a_1(\gamma + 1)} \left(u_1 - \frac{x - x_0}{t} \right) \right]^{\frac{2\gamma}{\gamma - 1}} \tag{61}$$

$$u_3 = \frac{2}{\gamma + 1} \left[a_1 + \frac{1}{2}(\gamma - 1)v_1 + \frac{x - x_0}{t} \right] \tag{62}$$

5.1.3 Contact Discontinuity

Region 3 extends $tV_{\text{tail}} < x - x_0 < tV_{\text{contact}}$ and Region 4, $tV_{\text{contact}} < x - x_0 < tV_{\text{shock}}$, where $V_{\text{contact}} = u_3 = u_4$.

Using the Rankine-Hugoniot conditions, $\Delta\mathbf{F} = V\Delta\mathbf{U}$ where V is the velocity of the discontinuity and $\Delta\mathbf{U}$ and $\Delta\mathbf{F}$ are the difference in state variables and their flux across the discontinuity correspondingly, we can determine that across the contact discontinuity, velocity and pressure remains the same. Here the speed left of the contact discontinuity is derived by applying the jump conditions along with the Riemann invariant conditions.

$$u_3 = u_1 - \frac{2a_1}{\gamma - 1} \left[\left(\frac{P_3}{P_1}^{\frac{\gamma - 1}{2\gamma}} \right) - 1 \right] \tag{63}$$

Similarly for the region to the left of the shock wave,

$$u_4 = u_5 - (P_4 - P_6)\sqrt{\frac{A_5}{P_4 + B_5}} \tag{64}$$

Where $A_5 = 2/\rho_5/(\gamma - 1)$ and $B_5 = P_5(\gamma - 1)/(\gamma + 1)$. Given that, $u_3 = u_4 = u^*$ and $P_3 = P_4 = P^*$, we can subtract (63) and (64) for an expression for P^*

$$(P^* - P_5)\sqrt{\frac{A_5}{P_4 + B_5}} + \frac{2a_1}{\gamma - 1}\left[\left(\frac{P_3}{P_1}^{\frac{\gamma-1}{2\gamma}}\right) - 1\right] + u_5 - u_1 = 0 \tag{65}$$

The above can only be solved numerically to produce the terms $P_3 = P_4 = P^*$. Assuming that the gas in consideration is ideal, we have,

$$\rho_3 = \rho_1 \left(\frac{P_3}{P_1}\right)^{\frac{1}{\gamma}} \tag{66}$$

$$\rho_4 = \rho_6 \left(\frac{P_5(\gamma - 1) + P_4(\gamma + 1)}{P_4(\gamma - 1) + P_5(\gamma + 1}\right) \tag{67}$$

5.1.4 Shock

Region 5 is defined by $x - x_0 > tV_{\text{shock}}$ where the velocity of the shock is,

$$V_{\text{shock}} = u_5 + a_5\sqrt{\frac{(\gamma + 1)P_4}{2\gamma P_5} + \frac{\gamma - 1}{2\gamma}} \tag{68}$$

and $a_5 = \sqrt{\gamma P_5/\rho_5}$ is the local speed in region 5. The terms ρ_5, P_5, u_5 are as discussed previously.

5.1.5 Test Problems

The initial conditions for the Sod Problem are

$$U_L = \begin{bmatrix}\rho_L \\ P_L \\ u_L\end{bmatrix} = \begin{bmatrix}1.0 \\ 1.0 \\ 0.0\end{bmatrix}, \quad U_R = \begin{bmatrix}0.125 \\ 0.1 \\ 0.0\end{bmatrix}$$

The initial conditions for the Lax problem are,

$$U_L = \begin{bmatrix}0.445 \\ 3.56259 \\ 0.311\end{bmatrix}, \quad U_R = \begin{bmatrix}0.5 \\ 0.571 \\ 0.0\end{bmatrix}$$

Solutions of the above are demonstrated in the following figure.

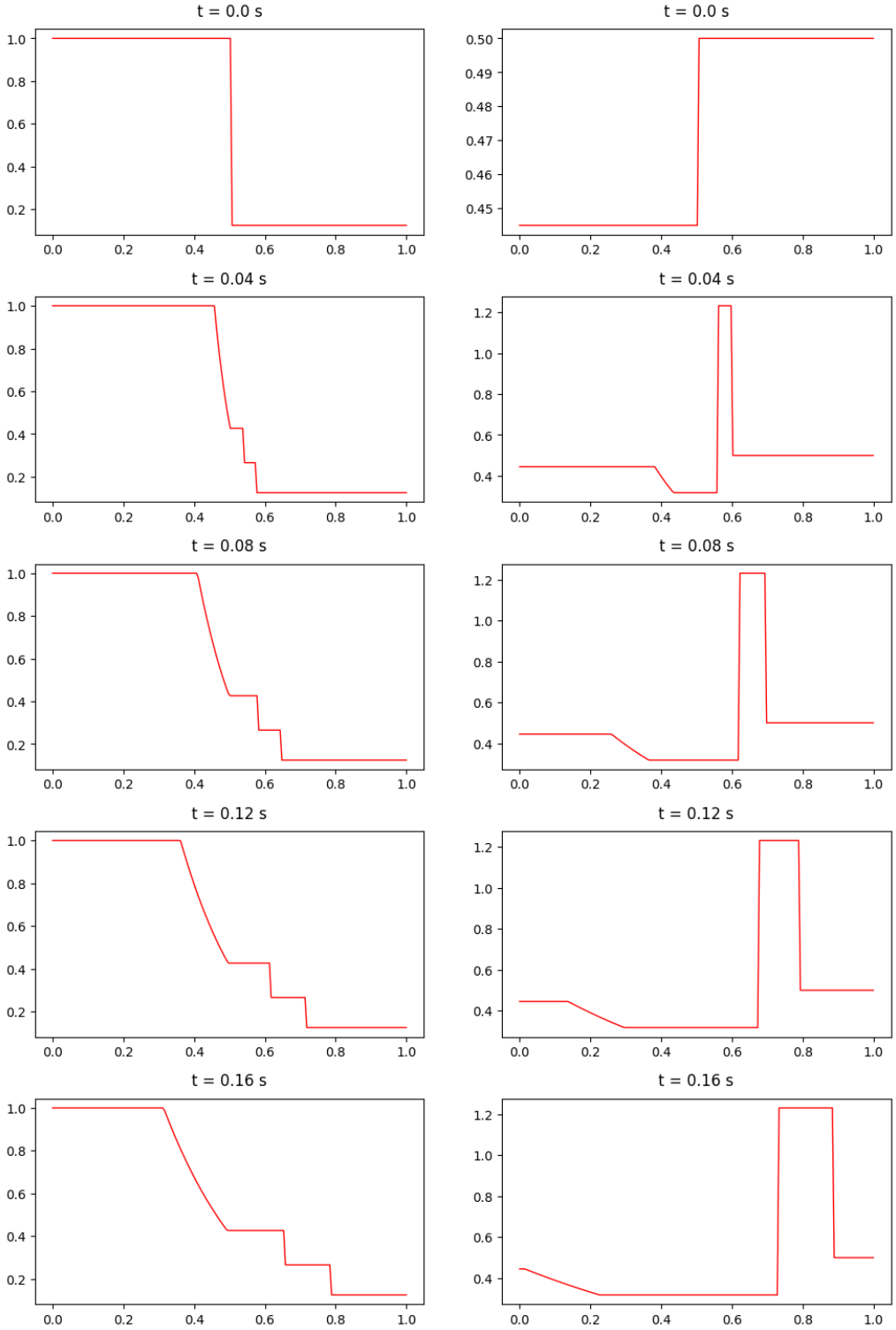

Figure 24: Density plotted for the Sod and Lax problems respectively for increasing timesteps

References

[1] E. F. Toro, *Riemann Solvers and Numerical Methods for Fluid Dynamics*, Springer, pp. 87-90, 1999. https:.//doi.org/10.1007/b79761

[2] G. A. Sod, A survey of several finite difference methods for systems of nonlinear hyperbolic conservation laws, *J. Comp. Phys*, vol. 27, no. 1, pp. 1-31, 1978. https://doi.org/10.1016/0021-9991(78)90023-2

[3] V. V. Rusanov, The calculation of the interaction of non-stationary shock waves and obstacles, *USSR Comp. Math. Math. Phys*, vol. 1, no. 2, pp. 314-320, 1962. https://doi.org/10.1016/0041-5553(62)90062-9

[4] R. D. Richtmyer, A Survey of Difference Methods for Non-Steady Fluid Dynamics, *NCAR Technical Notes 63-2*, 1962.

[5] R. W. MacCormack, The Effect of Viscosity in Hypervelocity Impact Cratering, *Frontiers of Comp. Fluid Dynam.*, 2002. https://doi.org/10.1142/9789812810793_0002

[6] A. Harten, G. Zwas, Self-adjusting hybrid schemes for shock computations, *J. Comp. Phys*, 1972. https://doi.org/10.1016/0021-9991(72)90012-5

[7] H. Nessyahu, E. Tadmor, Non-oscillatory central differencing for hyperbolic conservation laws, *J. Comp. Phys*, vol. 87, no. 2, pp. 408-463, 1990. https://doi.org/10.1016/0021-9991(90)90260-8

[8] A. Kurganov, E. Tadmor, New High-Resolution Central Schemes for Nonlinear Conservation Laws and Convection–Diffusion Equations, *J. Comp. Phys*, vol. 160, no. 1, pp. 241-282, 2000. https://doi.org/10.1006/jcph.2000.6459

[9] F. D. Lora-Clavijo, J. P. Cruz-Perez, F. Siddhartha Guzman, and J. A. Gonzalez, Exact solution of the 1D riemann problem in Newtonian and relativistic hydrodynamics, *Revista Mexicana de Fisica E*, 59, pp. 28–50, 2013